The Shielding-Effectiveness Based Magnetic Field Shielding Theory and Its Application in Mobile Payment Systems

Yejun He, Jiefeng Ao, Jie Yang, Xiaorong Tang
Shenzhen Key Lab of Advanced Communications and Information Processing
College of Information Engineering, Shenzhen University, 518060, China
Email: heyejun@126.com; http://cie.szu.edu.cn/heyejun

***Abstract*—In this paper, we firstly introduce theory of magnetic coupling. Then, the shielding-effectiveness based electromagnetic shielding theory is studied, and the effectiveness of shielding materials to the coupling process is analysed in mobile payment systems. Simulation results show that when the feed frequency is low, plastic and lithium cell cause almost no attenuation to the magnetic field. If a shielding material is common metal, the magnetic field intensity is reduced to 20%-70% of the original. In the low frequency condition, the time-varying magnetic field produced by the transmitting coil is very stable and can resist the external interference. A convenient simulation software to calculate magnetic field coupling with shielding materials is also developed.**

Keywords—shielding-effectiveness; electromagnetic shielding; mobile payment; transmitting coil; coupling coil

I. INTRODUCTION

Mobile payment is a very important part of the construction of "smart earth" and a service method by which the user pays the goods or the services through a mobile phone. Therefore, it is also known as "mobile phone payment". There are three different mobile payments at home and abroad: a contactless NFC (near field communication) based on 13.56 MHz (Japan, South Korea, France and other countries introduced) [1-4], an affixed-chip card scheme based on the frequency of 13.56 MHz (a 13.56 MHz card is sticked on the back cover of mobile phone) [5], and a RFID-SIM card program based on the frequency of 2.4 GHz (independently researched and developed by Nationz Technologies Co. Ltd., Shenzhen).

RFID smart labels are affixed to the battery shell of mobile phone to save space. The RFID mobile phones are widely used in Japan and other countries. It is very difficult to integrate mobile phone with SIM for the affixed-chip card method, so its application is limited. Moreover, with the extensive application of RFID, the interference problem is becoming more and more serious. The interference is mainly manifested in two aspects: (1) the identifying distance is far lower than the designed distance; (2) the reader or the electronic tag does not respond, which will result in invalid read. In the actual application of high frequency RFID electronic label, we need to consider the position where 13.56 MHz RFID electronic label is attached. Due to the large size of the label and the limited actual space allowed plus other factors, electronic label needs to be directly attached to the surface of the metal or the location near the metal device. Thus, in the process of recognition, the electronic label is vulnerable to the vortex on the stamping shell of the aluminum battery, which will result in a small effective reading distance of RFID labels or failure of response.

In view of this, we put forward a new scheme and make theoretical research, system simulation and field test of this scheme. Research shows that this mobile phone payment scheme has lots of advantages such as safety, good robustness, low cost and strong capacity of resisting disturbance. The basic principle of this scheme is based on the electromagnetic induction between the reader coil (called the transmitting coil in this paper) and the transponder coil (called the coupling coil in this paper), which is the same as the RFID technology based on the 125 kHz or 13.56 MHz. When the transponder is close to the alternating magnetic field generated by the reader, the induced voltage will be generated on the transponder coil. When the transponder is close enough to the reader coil such that the induced voltage on the transponder reaches a threshold value, the information authentication is activated and the swiping card action is completed. Because the reader coil is integrated on a SIM card of a mobile phone, a battery and a cover of the mobile phone also need to be mounted outside the SIM card. The two materials are likely to affect the coupling process. Experiments have proved that, a different permeability of shielding material (i.e., the actual battery or the mobile phone cover) between the reader and the transponder has different effects on the entire coupling process.

The rest of this paper is organized as follows: Section II analyzes the coupling voltage when there is no shielding material between a reader and responder. Section III introduces the electromagnetic shielding theory based on shielding effectiveness. Section IV presents simulation results and conclusion.

II. THEORY OF MAGNETIC COUPLING

Fig.1 is a block diagram of the coupled system with a circular transmitting coil. The resistance of a circular transmitting coil is

$$R = N_1 \rho \frac{L}{S} = N_1 \rho \frac{2a}{{a_0}^2} \tag{1}$$

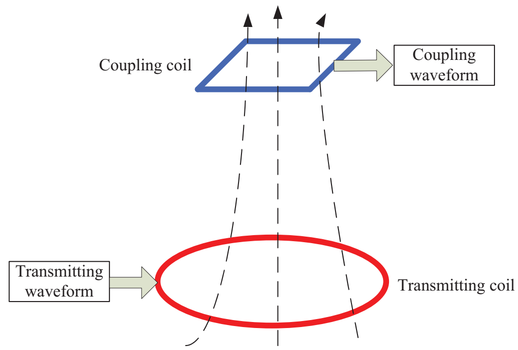

Fig. 1. The coupling model without a shielding material near circular coil.

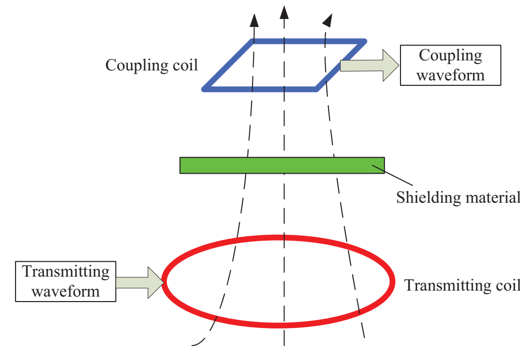

Fig. 2. Schematic diagram with a specific shielding material.

where ρ is the resistivity, a is the circular coil (or the transmitting coil) radius, a_0 is the conductor radius, N_1 is the number of turns of the transmitting coil.

When the transmitting waveform is an AC voltage, the current in the transmitting coil is

$$I = \frac{U}{\sqrt{R^2 + (L\omega)^2}} \tag{2}$$

where the self-inductance coefficient [6] is

$$L = {N_1}^2 \mu_0 a (\ln \frac{8a}{a_0} - 1.75) \tag{3}$$

whrer μ_0 is the permeability of vacuum and is equal to $4\pi \times 10^{-7}$ H/m, U is the voltage in the transmitting coil.

Since the magnetic field intensity at a distance of z along the axis direction of circular transmitting coil (the origin of coordinates is at the transmitting coil center) is given by

$$H = \frac{IN_1a^2}{2(a^2+z^2)^{3/2}}, \tag{4}$$

the magnetic flux density is given by

$$B = \mu_0 H = \frac{\mu_0 I N_1 a^2}{2(a^2+z^2)^{3/2}} \tag{5}$$

When $z^2 \gg a^2$,

$$B = \mu_0 H \approx \frac{\mu_0 I N_1 a^2 z^{-3}}{2} \tag{6}$$

From (5), when z is big enough compared with the coil radius a, the magnetic flux density goes down exponentially with the height z. The instantaneous induced voltage u on the coupling coil is as follows:

$$\begin{aligned} u &= -\frac{d\Psi_{21}}{dt} = -\frac{d(N_2\phi_{21})}{dt} \\ &= -N_2 \frac{d}{dt}[\int \frac{\mu_0 i_1 N_1 a^2}{2(a^2+z^2)^{3/2}} ds] \\ &= -[\frac{\mu_0 N_1 N_2 a^2 (a_1 b_1)}{2(a^2+z^2)^{3/2}}]\frac{di}{dt} \\ &= -M\frac{di}{dt} \end{aligned} \tag{7}$$

where Ψ_{21} is the mutual flux chain, i is the excitation current on the transmitting coil, ϕ_{21} is the magnetic flux across the coupling coil produced by i, a_1 is the length of the coupling coil, b_1 is the width of the coupling coil, z is the distance between the transmitting coil and the coupling coil, M is the mutual inductance between the transmitting coil and the coupling coil, N_2 is the number of turns of the coupling coil. The minus sign in the equation suggests that the mutual inductance voltage and the mutual flux chain on the coupling coil do not meet the right-handed helical rule. When the excitation source is a voltage source, the current I can be calculated by $I = U/\sqrt{R^2 + (L\omega)^2}$.

III. Electromagnetic Shielding Theory Based on Shielding Effectiveness

As shown in Fig. 2, a specific shielding material is placed between the transmitting coil and the coupling coil. This section mainly discusses how the different shielding materials influence the magnetic coupling. In fact, some shielding materials may completely shield the magnetic field, and some materials have no effect on the magnetic field coupling. So it is necessary for us to study the influence of the specific shielding materials. This paper mainly uses the electromagnetic shielding theory for analyzing.

"Shielding" is usually referred to as electromagnetic shielding. Electromagnetic shielding is the process of reducing the electromagnetic field in a space by blocking the field with metal or magnetic materials. In other words, the propagation of an electromagnetic wave from one region to another region can be effectively controlled by isolating the electromagnetic wave. Electromagnetic shielding generally refers to the shielding of an alternating electromagnetic field with frequency larger than 10 kHz [7]. In an alternating electromagnetic field, the electric field and the magnetic field always exist at the same time. Therefore we must consider the shielding for the electric field and the shielding for the magnetic field. However, due to the difference in frequency, the effective interference area of an alternating electromagnetic field is different. When the frequency is low, the electromagnetic interference occurs in the near field, which is suited to the near field shielding theory

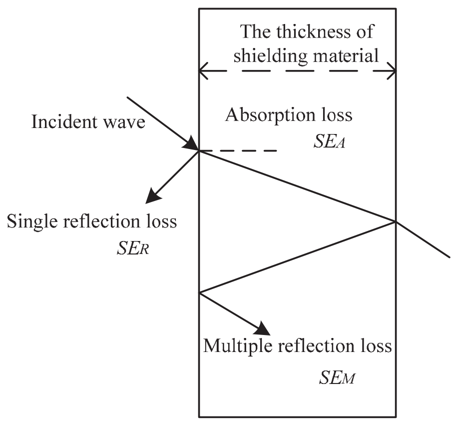

Fig. 3. The shielding effectiveness of the shield.

based on electric dipole and magnetic dipole. In the near field, because of the difference in the interference sources, the ranges of the electric field and the magnetic field are different. When the interference source has a high voltage and a low current, we can consider only the electric field shielding and ignore the magnetic shielding. On the other hand, when the interference source has a low voltage and a high current, we can consider only the magnetic field shielding and ignore the electric field shielding.

There are lots of explanations about the electromagnetic shielding mechanism such as the eddy current theory, the electromagnetic field theory, and the transmission line theory. Among these methods, the transmission line theory is widely used because of its simple calculation, high precision and ease to understand.

As shown in Fig. 3, the transmission line theory regards the shield as a section of a transmission line. When the radiation field passes through the shield, a part of the radiation field is reflected on the outer surface and the rest penetrates into the shield and transmits forward. During the transmission, the electromagnetic wave is continuously attenuated by the shield and is reflected and projected many times between the two interfaces of the shield. Therefore, the electromagnetic shielding mechanism includes the single reflection loss on the surface of the shield, the absorption loss of the shielding material and the multiple reflection loss inside the shield.

The electromagnetic shielding studied in this paper refers only to the magnetic shielding. The shielding effectiveness (SE) in decibels (dB) can be defined as the ratio of H_0 to H_s as described by

$$SE = 20lg\frac{|H_0|}{|H_s|} \tag{8}$$

where H_0 and H_s are the magnetic field intensities without and with shielding, respectively. From (8), we can get the magnetic field intensity H_s:

$$H_s = H_0 10^{-\frac{SE}{20}} \tag{9}$$

where $10^{-\frac{SE}{20}}$ is the attenuation factor of the magnetic field.

At present, the common calculation formula for the shielding effectiveness of uniform shielding materials is the Schelkunoff formula. This formula is based on the transmission line model and is suitable for flat conductor shielding material. The formula is given by

$$SE = SE_A + SE_R + SE_M(\mathrm{d}B) \tag{10}$$

where SE_A is the absorption loss of a shielding material in dB, SE_R is single reflection loss on the surface of the shield material in dB, SE_M is multiple reflection loss inside the shield material in dB. The three terms are written as [7]:

$$SE_A = 131.43t\sqrt{f\mu_r\sigma_r} \tag{11}$$

$$SE_R = 20lg(5.35r\sqrt{\frac{f\sigma_r}{\mu_r}} + 0.354 + \frac{1.17\times10^{-2}}{r}\sqrt{\frac{\mu_r}{f\sigma_r}}) \tag{12}$$

$$SE_M = 10lg[1-2\times10^{-0.1\times SE_A}\times cos(0.23SE_A)+10^{-0.2\times SE_A}] \tag{13}$$

where f is the frequency of the electromagnetic wave in Hz; t is the thickness of a shielding material in meters; r is the distance between the source and the shielding material in meters; μ_r is relative permeability of a shielding material relative to free space; σ_r is relative electrical conductivity (relative to copper). If SE_A is greater than 15 dB, SE_M is negligible.

Note that the single reflection loss of most of materials SE_R is very small, and that for the electromagnetic shielding layer, multiple reflection loss SE_M can be neglected compared to the absorption loss SE_A. Therefore, the shielding effectiveness of the electromagnetic shielding layer SE is approximately equal to SE_A, which can be calculated by formula (11).

From (9) we know that the attenuation factor is $10^{-\frac{SE}{20}}$. Since the attenuation of the magnetic field is accompanied in the attenuation of the coupling coil, the coupling voltage with a shielding material is given by:

$$\begin{aligned} V &= -[\frac{\mu_0 N_1 N_2 a^2 S_1}{2(a^2+z^2)^{3/2}}]\frac{di}{dt}10^{-\frac{SE}{20}} \\ &= -[\frac{\mu_0 N_1 N_2 a^2 S_1}{2(a^2+z^2)^{3/2}}]\frac{di}{dt}10^{-\frac{131.43t\sqrt{f\mu_r\sigma_r}}{20}} \end{aligned} \tag{14}$$

where S_1 is the area of the coupling coil, S_2 is the area of the shielding material, z is the distance between the transmitting coil and the coupling coil.

IV. Simulation Results and Conclusion

We have simulated the scenario with and without a shielding material. The parameters of the transmitting coil are: circular coil, the radius is 89.25 mm, the number of turns is 110, and copper wire diameter is 0.6 mm. The parameters of the coupling coil (transponder) are: rectangular coil, the length is 24 mm, the width is 14 mm, and the number of turns is 4. The distance between the transmitting coil and the transponder coil is 124 mm. The relative permeability and electrical

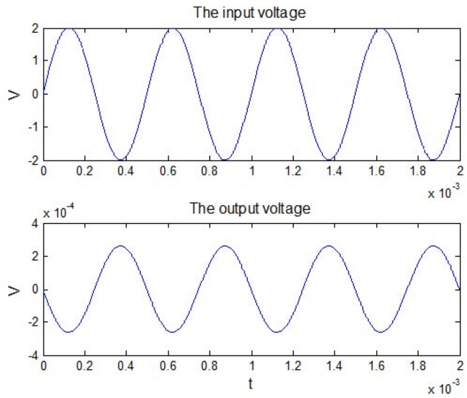

Fig. 4. The input waveform and the coupling wave without shelter.

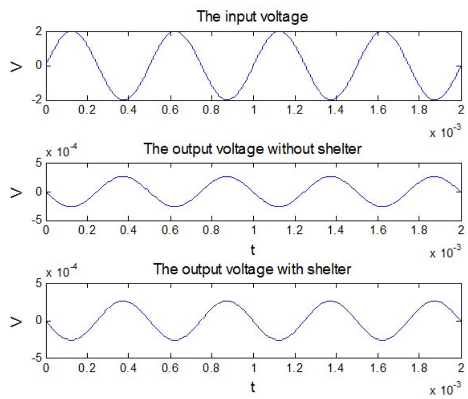

Fig. 5. The input waveform, the coupling waveform without shelter as well as the coupling waveform with shelter (plastic shield).

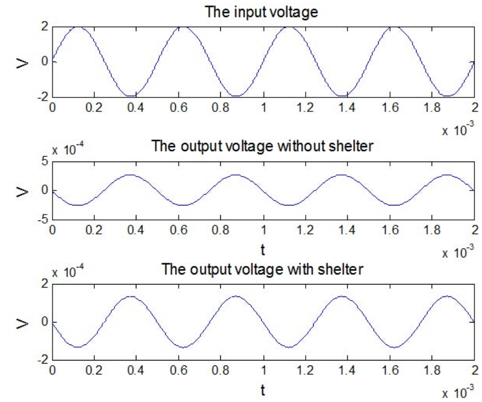

Fig. 6. The input waveform, the coupling waveform without shelter as well as the coupling waveform with shelter (copper shield).

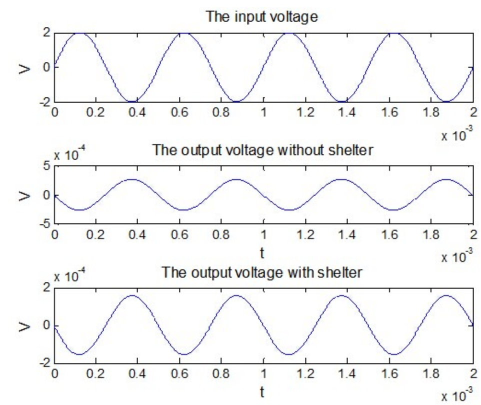

Fig. 7. The input voltage waveform, the coupling waveform without shelter as well as the coupling waveform with shelter (aluminum shield).

conductivity of plastic are 1 and 10^{-6} S/m, respectively; those of copper are 1 and 5.8×10^7 S/m, respectively; and those of aluminum are 1 and 3.4×10^7 S/m, respectively. The input excitation voltage of the transmitting coil (located in the reader) is sinusoidal with an amplitude of 2 V and a frequency of 2 kHz (i.e. a period of 0.5×10^{-3} s). The input waveform is the first wave as shown in Fig. 4 and the coupling waveform when there is no shelter (shield) is the second wave as shown in Fig. 4. When the shield exists, the waveforms are shown in Figs. 5 to 7.

From Fig. 4 and Fig. 5 we can see that the input AC voltage is 2 V, the coupling voltage amplitude without shelter is about 263 uV, and the coupling voltage with shelter (plastic shield) is about 263 uV. The results suggest that a plastic shield does not affect the coupling voltage.

From Fig. 6 we find that the input AC voltage is 2 V, the coupling voltage amplitude without shelter is about 263 uV, and the coupling voltage with shelter (copper shield) is about 133 uV. The results suggest that the coupling voltage with the copper shield is reduced to half of the coupling voltage amplitude without shelter.

From Fig. 7 we get that the input AC voltage is 2 V, the coupling voltage amplitude without shelter is about 263 uV, and the coupling voltage with shelter (aluminum shield) is about 156 uV. The results suggest that the coupling voltage with aluminum shield is reduced to 60% of the coupling voltage amplitude without shelter.

The simulation results above show that plastic does not have apparent effect on the mobile-payment system. However, the effect of copper and aluminum shield is obvious, reducing the magnetic field intensity to the 50%-60% of the original. The results show that shield materials with small conductivity such as plastic has a little effect on the coupling process, which can be neglected. But for shield materials with large conductivity such as metal, the effect cannot be ignored. In practical applications, we should also consider this problem in order to avoid “no response” in the mobile-payment system for some mobile phones.

In addition, we developed a convenient simulation software to calculate magnetic field coupling with shielding materials. Fig. 8 illustrates our simulation interface. We are launching a mobile payment application in China by means of our technologies. Fig. 9 describes a practical reader with a transmitting coil while a coupling coil is integrated in SIM card.

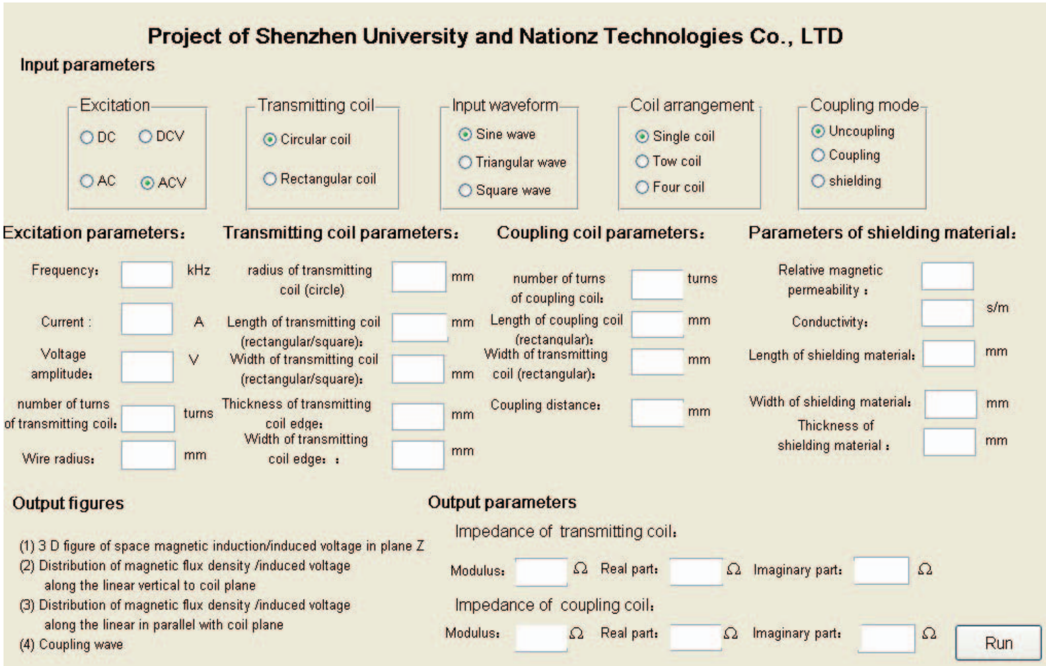

Fig. 8. Software interface for magnetic field coupling.

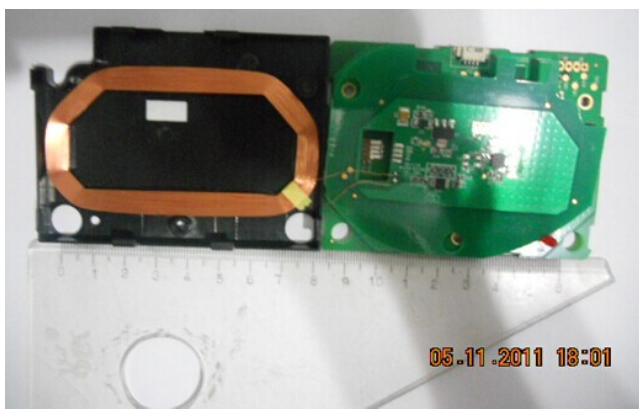

Fig. 9. Practical reader with a transmitting coil.

Acknowledgement

This work was supported in part by the Foundation of Nationz Technologies Co, Ltd., the National Natural Science Foundation of China under Grants No. 61372077 and No. 60972037, the Fundamental Research Program of Shenzhen City under Grants No. JC201005250067A and No. JCJY20120817163755061, the International Cooperative Program of Shenzhen City under Grant No. ZYA201106090040A and the Technical Research and Development Program of Shenzhen City under Grant No. CXZZ20120615155144842.

References

[1] A. Shameli, A. Safarian, A. Rofougaran, M. Rofougaran, J. Castaneda, F. De Flaviis, “A UHF Near-Field RFID System With Fully Integrated Transponder,” *IEEE Transactions on Microwave Theory and Techniques*, vol. 56, no. 5, pp. 1267-1277, May 2008.

[2] Wei-Dar Chen, Keith E. Mayes, Yuan-Hung Lien, Jung-Hui Chiu, “NFC Mobile Payment with Citizen Digital Certificate,” *2011 The 2nd International Conference on Next Generation Information Technology (ICNIT)*, pp. 120-126, 2011.

[3] Roy Want, “Near Field Communication,” *IEEE Pervasive Computing*, vol. 10, no. 3, pp. 4-7, July-Sept., 2011.

[4] J. Morak, H. Kumpusch, D. Hayn, R. Modre-Osprian, G. Schreier, “Design and Evaluation of a Telemonitoring Concept Based on NFC-Enabled Mobile Phones and Sensor Devices,” *IEEE Transactions on Information Technology in Biomedicine*, vol. 16, no. 1, pp. 17-23, January 2012.

[5] M. Gebhart, R. Neubauer, M. Stark, D. Warnez, “Design of 13.56 MHz Smartcard Stickers with Ferrite for Payment and Authentication,” *2011 Third International Workshop on Near Field Communication*, pp. 59-64, 2011.

[6] W. Grover Fredesrick. Inductance Calculations: Working Formulas and Tables. Dover Publications, Inc., New York, 1946.

[7] ShunHua Liu, Junmin Liu, Xinlong Dong. The electromagnetic wave shielding and absorbing materials (in Chinese). Chemical Industry Press, 2007.